PHYSICAL REVIEW B **70**, 081401(R) (2004)

Hydrogen and carbon effects on Al_2O_3 surface phases and metal deposition

Xiao-Gang Wang and John R. Smith
Delphi Research Labs, Shelby Township, Michigan 48315, USA
(Received 24 May 2004; published 3 August 2004)

Substantial effects of combinations of H and C impurities on wetting of metals on α-Al_2O_3(0001) have been found from first principles. An *ab initio* surface phase diagram for H and C on the alumina surface reveals six distinct surface phases, consistent with the observed stability of H and C on Al_2O_3 surfaces. These different surface phases exhibit a variety of adhesion strengths with Cu and Co, and correspondingly different wetting behaviors. These results are consistent with the variety of wetting characteristics observed experimentally.

DOI: 10.1103/PhysRevB.70.081401 PACS number(s): 68.35.Dv, 68.03.Hj, 68.35.Np, 68.47.Gh

Alumina surfaces with and without metal overlayers have been extensively examined in recent years[1–15] since they are important for catalyst supports, corrosion resistance, optical electronic components, and for thermal management of electronic components. Differing experimental results have been reported for metal wetting behavior on alumina, however. Here, we report for the first time significant effects of mixtures of the commonly found impurities C and H on metal wetting, which help one to understand the variety of experimental results.

C and H interfacial and surface impurities can arise from the presence of hydrocarbons, water vapor, and other ambient gases such as CO_2. Ahn and Rabalais[2] observed that hydrogen could be stable on alumina surfaces even after annealing at 1100 °C under ultrahigh-vacuum conditions. Niu *et al.*[13] observed that carbon is also so stable that it is found on the Al_2O_3(0001) surface after annealing at 1100 K in a 5×10^{-6} torr partial pressure of O_2. This observed stability of H and C is consistent with our findings of stable surface phases of combinations of C and H, as described below.

There is some evidence in the literature of the effect of H on alumina surface structures and metal wetting. In the absence of H and other impurities, it has been found[5,6,9,14,15] that the aluminum-terminated Al_2O_3(0001) surface is the ground-state configuration (i.e., it has the lowest surface energy). The presence of hydrogen in the environment results in the oxygen-terminated surface becoming stable.[3,5,7,14,15] Such a hydrogen-terminated surface can play a bridging role in the formation of the oxygen-terminated alumina/metal interface,[10] and the laminar growth of the metal on the alumina surface.[11]

No results of *ab initio* computations on the effect of C impurities or mixtures of C and H impurites on the structure of the alumina surface, or on metal wetting behavior have been reported in the literature as yet, however. These are the subjects that will be addressed in this manuscript.

An *ab initio* full-potential linearized augmented plane-wave method (FP-LAPW) was employed to obtain a surface phase diagram for H and C on an alumina surface. The phase diagram offers direct information about the nature of the alumina surface structures attainable. The oxygen-terminated α-Al_2O_3(0001) surface, stabilized as discussed above by H, is treated in the presence of C and C/H mixtures. Our results reveal six distinct surface configurations that can form in the presence of H and C. A variety of metal wetting behaviors are found over these different surface configurations.

We define the Gibbs free energy of formation ΔG for a surface phase x relative to the 3H-terminated surface phase (each surface O atom bonded to a H atom), as follows:

$$\Delta G = G_x(n_x^{\mathrm{C}}, n_x^{\mathrm{H}}) - G_{3\mathrm{H}}(n^{3\mathrm{H}}) - n_x^{\mathrm{C}}\mu_{\mathrm{c}} - (n_x^{\mathrm{H}} - n^{3\mathrm{H}})\mu_{\mathrm{H}}. \quad (1)$$

Here, $G_x(n_x^{\mathrm{C}}, n_x^{\mathrm{H}})$, and $G_{3\mathrm{H}}(n^{3\mathrm{H}})$ are the free energies for the Al_2O_3 systems with the x and 3H-terminated surface phases, respectively. n_x^{C} and n_x^{H} are the numbers of C and H atoms found on the surface phase x, and $n^{3\mathrm{H}}$ is the number of H atoms found on the 3H-terminated surface phase. μ_{C} and μ_{H} are the reservoir chemical potentials of C and H. Here, the reservoir is the source of the impurity H and C atoms, and it might be the ambient gas or the bulk alumina, or both. The C and H impurity atoms may segregate from the alumina bulk, or they may arrive from adsorption and dissociation of ambient H_2O and CO_2 gases.

The first two terms on the right-hand side of Eq. (1) are written as $G_x(n_x^{\mathrm{C}}, n_x^{\mathrm{H}}) - G_{3\mathrm{H}}(n^{3\mathrm{H}}) = E_x^{\mathrm{total}} - E_{3\mathrm{H}}^{\mathrm{total}} + P\ \Delta V + \Delta F(T)$. Here, $E_x^{\mathrm{total}}$and $E_{3\mathrm{H}}^{\mathrm{total}}$ are the total energies of the x and 3H-terminated surface systems at $T=0$ K, respectively, both of which can be obtained from our FP-LAPW calculations. It has been shown[16] that the $P\ \Delta$V term can be safely neglected. Following Lodziana *et al.*,[14] who showed for hydroxylated alumina surfaces that the vibrational surface free energy can be an order of magnitude larger than the surface configurational energy, we take $\Delta F_V(T)$ to be the difference between the vibrational surface free energies of the two surface systems. One can reasonably assume that $\Delta F_V(T)$ is dominated by the vibrational contributions of the surface impurity complexes, such as O-H, O-C, H-C, etc. It has been shown[4,17] that the molecular vibrational frequencies mainly depend on the local bonding character and not on the environment. For example, the vibrational frequency for the surface O-H is 3720 cm^{-1},[4] and that for the O-H in water is 3728 cm^{-1} (stretching vibration). Assuming conservatively that vibrational frequencies change by no more than ±10% due to changes in the environment, we find, for example, that for the 2(H-O)-terminated surface system, the ratio $\|\Delta F_V(T)\|/\|(E_{2\mathrm{H}}^{\mathrm{total}} - E_{3\mathrm{H}}^{\mathrm{total}})\|$ is less than 0.013 for temperatures

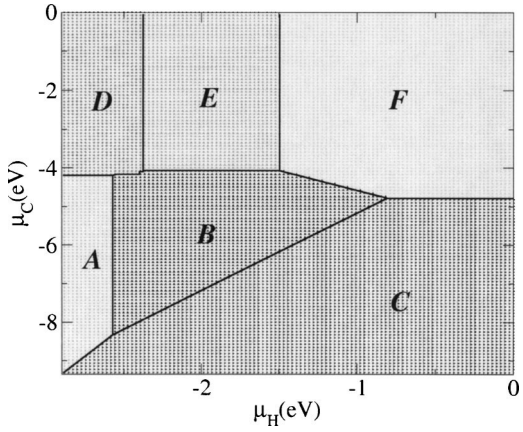

FIG. 1. (Color online) Phase diagram for the $Al_2O_3(0001)$ surface in the presence of H and C as a function of μ_H and μ_C. $\mu_H=0$ corresponds to H_2 molecules and $\mu_C=0$ corresponds to interstitial C atoms in the Al_2O_3 bulk. The 1C-terminated surface is found in region ***A***, the 1(H-C)-terminated surface in region ***B***, the 3H-terminated surface in region ***C***, the 3C-terminated surface in region ***D***, the (1H-3C)-terminated surface in region ***E***, and the 3(H-C)-terminated surface in region ***F***. Their surface structure configurations are shown in Fig. 2.

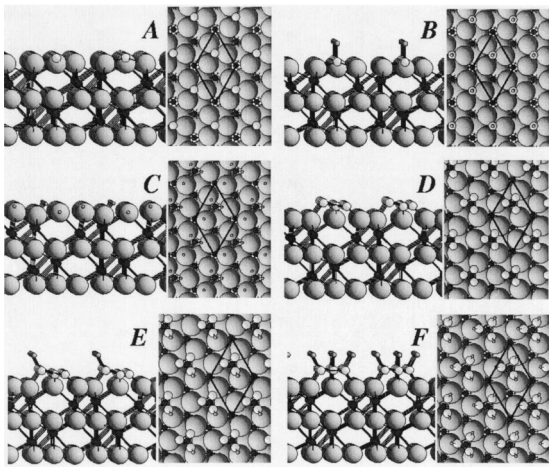

FIG. 2. (Color online) Principal oxygen-terminated $Al_2O_3(0001)$ surface configurations in the presence of H and C. The large balls represent O atoms, the midsize black balls Al atoms, the midsize gray balls C atoms, and the small balls H atoms. ***A***, ***B***, ***C***, ***D***, ***E***, and ***F*** indicate the same surfaces as they do in Fig. 1. The surface unit cell is plotted in the figure.

in the range of 0–2000 K. The variation of ΔG with T and P in Eq. (1) is then primarily from the temperature and pressure dependencies of the chemical potentials of H and C. Then, Eq. (1) can be approximately written as: $\Delta G \approx \Delta G(\mu_C, \mu_H)$, and one can obtain the surface phase diagram in terms of μ_C and μ_H.

Now the details of our calculational methods are discussed. The $(1\times1)Al_2O_3(0001)$ surfaces are modeled by a slab, which consists of a finite number of layers of infinite extent in the plane of the surface. The slabs are repeated periodically along the [111] direction, and separated by more than 10 Å of vacuum. Each slab contains four oxygen layers and six or eight Al layers, depending on the surface termination. At equilibrium, the total energy is minimized and forces on all atoms are below 26 meV/Å. In our total-energy and force calculations, the exchange-correlation potential follows the generalized gradient approximation (GGA) of Perdew *et al.*,[18] and the FP-LAPW method is employed to solve the Kohn-Sham equations.[19–22] The GGA in the FP-LAPW calculations has been tested[9,23,24] for metal-oxide surfaces and interfaces against the less accurate local-density approximation (LDA) and against experimental results, where available for surface and interface energies, and relaxed atomic positions. The tests show that trends and conclusions are not affected by employing the more accurate GGA in place of the LDA.[9,23,24]

Next, the results of our computations are presented. Thirty-six (1×1) impurity structures of the form xH-yC were treated, where $0\leqq x\leqq5$, and $0\leqq y\leqq5$ and x and y are the number of H or C atoms per unit cell, respectively, including possible subsurface impurity structures. Figure 1 shows the surface phase diagram for the $Al_2O_3(0001)$ surface in the presence of C and H impurities. The six lowest-energy distinct surface configurations are depicted in Figs. 1 and 2, including both the top and side views. The existence of these configurations depends on the reservoir chemical potentials. At a relatively low chemical potential of C, and a high chemical potential of H, the 3H-terminated surface phase becomes stable, as expected. An increase of the C chemical potential makes the 3(H-C)-terminated phase the stable phase. At relatively low chemical potentials of H and C, the 1C-terminated surface phase become stable, as shown in Fig. 1. In general, one can see that as these reservoir chemical potentials μ_C and μ_H decrease, the number of C and H atoms per surface unit cell at the stable surface decreases. It is not difficult to understand this, since with the decrease of the reservoir chemical potentials, there would be less energy lowering (or perhaps an energy increase) associated with the taking of an H or C atom out of the corresponding reservoir and binding it to the surface. These stable C-containing surface configurations we have found are consistent with the surface C observed[13] on $Al_2O_3(0001)$, even after annealing.

Note that there are no subsurface H or C, and there are no xH-2C and 2H-xC terminations among the six lowest-energy configurations. C and H on the O-terminated Al_2O_3 surface tend to fill the sites available on the Al_2O_3 surface, and at the same time, fill the dangling bonds of the covalent impurities. These impurities can do so within only those discrete configurations shown. For example, for the 1(H-C)-terminated surface, the C atoms occupy the position of the topmost Al atoms of the clean Al-terminated surface, as shown at ***B*** in Fig. 2. The carbon atoms are bonded to the three oxygen nearest neighbors and the dangling bond of the carbon atoms are saturated by the hydrogen atoms.

This absence of the xH-2C and 2H-xC terminations does not of course imply that the experimentally observed surface coverage of either C or H is discontinuous. Rather, it just means that for the oxygen-terminated surface the C and H atoms that are there are found in only the local site configurations shown in Fig. 2. In Fig. 2, only the (1×1) cases are

shown, where all the local site configurations are filled. The alumina substrate has been observed experimentally to be (1×1) in air and in UHV at temperatures below about 1100 C (see, e.g., Refs. 2 and 8). The surface may fill continuously with C or H by occupying an increasing fraction of the sites shown, by containing varying amounts of more than one surface phase (e.g., more than one of the six phases shown in Figs. 1 and 2), or a combination of these conditions. Ideally, we would have carried out FP-LAPW computations for fractional monolayer coverages, but this is beyond the current capabilities of this very accurate, but computationally intensive, method.

Now that impurity effects on the alumina surface configurations have been determined, metal deposition on these configurations will be considered. There has been considerable experimental work done[11,25–34] on metal wetting of alumina surfaces. There are apparent discrepancies between results reported by the different groups, however. For example, x-ray photoelectron spectroscopy (XPS) experiments on the growth of thin films of Cu on an $Al_2O_3(0001)$ surface by Varma *et al.*[26] indicated that Cu initially forms uniform films up to a monolayer and, subsequently, clusters begin to form. Other studies[27–29] on Cu deposited on Al_2O_3 substrates also showed the initial layer-by-layer growth. But Wu *et al.*[30] carried out XPS and low-energy ion scattering experiments and reported that Cu grows as three-dimensional (3D) clusters on the Al_2O_3 surface, even at the lowest observable coverages, which is consistent with the results of other experiments.[31–33] Baumer and Freund[34] indicated that almost all metals deposited on alumina films form 3D islands. Chambers *et al.*[11] found that Co can grow on hydroxylated $Al_2O_3(0001)$ in a laminar fashion, however.[35]

One may consider the possibility that the discrepancies may originate from different Al_2O_3 surfaces [Figs. 1 and 2] being presented to the metals. As discussed above, there are six distinct types of stable $Al_2O_3(0001)$ surface phases in the presence of the common impurities C and H. The six surfaces presumably provide different wetting behavior for metal deposited on them. Layer-by-layer growth[36] will occur when

$$\Delta G_f = G_{fs}(P,T) - G_s(P,T) - N_m\,\mu_m(p_m,T) \leqslant 0, \qquad (2)$$

where G_{fs} is the free energy for the film-substrate system, G_s the free energy of the substrate, and N_m and μ_m the number and free energy of the metal atoms deposited. p_m is the partial pressure of the metal vapor. Based on the same arguments presented following Eq. (1), one can write $\Delta G_f \approx (E_{fs}^{\text{total}} - E_s^{\text{total}}) - N_m\,\mu_m(p_m,T)$, where E_{fs}^{total} and E_s^{total} are the total energies of the film-substrate system and substrate, respectively. $\Delta G_f \leqslant 0$ means that complete wetting of the substrate is favorable.

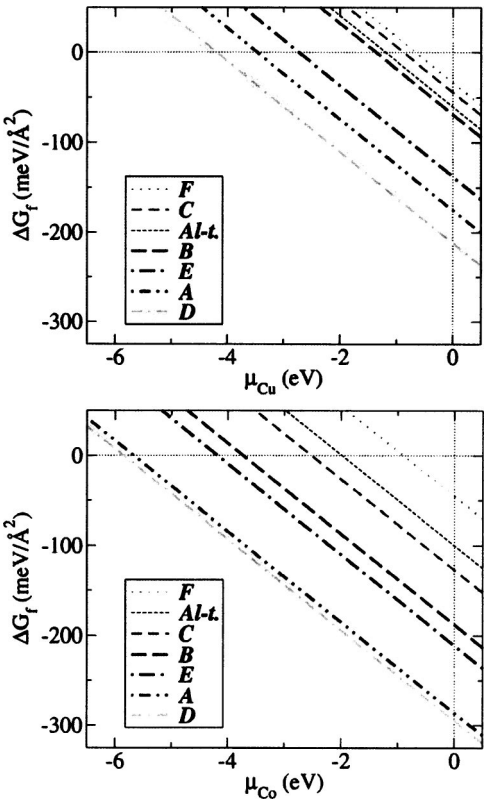

FIG. 3. (Color online) ΔG_f vs μ_{Cu} and μ_{Co}. $\mu_{Cu}=0$ corresponds to isolated Cu atoms, and $\mu_{Co}=0$ to isolated Co atoms. ***A***, ***B***, ***C***, ***D***, ***E***, and ***F*** indicate the same surfaces as they do in Fig. 2. *Al-t.* indicates the clean Al-terminated surface.

The effects of the alumina surface phases on metal wetting behavior will now be investigated for the wetting of Cu and Co. For this initial study, 1/3 ML of the metals (one metal atom for every three oxygen atoms in the outermost oxygen layer of the alumina), are deposited on the alumina substrates. For the Co adlayers, spin-polarized computations were done. Figure 3 exhibits the dependence of ΔG_f on the metal chemical potential $\mu_m(p_m,T)$. One can see that the different surface phases induce different wetting behaviors for the metals, Also the Cu wetting behavior is significantly different from the Co wetting behavior. Cu and Co have in common that the 3(H-C)-terminated surfaces [phase F, Figs. 1–3], wet these metals only over a relatively small range near the zero point of the metal chemical potentials. This is presumably due to the relatively high coverage of (H-C) at the alumina surface weakening the interaction between the metal atoms and surfaces.

TABLE I. Work of adhesion for 1/3 ML Cu and Co on the Al_2O_3 surfaces. The unit is J/m^2. ***A***, ***B***, ***C***, ***D***, ***E***, and ***F*** indicate the same surfaces as that they do in Fig. 1. *Al-t.* indicates the clean Al-terminated surface.

	F	***C***	***B***	***E***	***A***	***D***	*Al-t.*
Cu	0.24	0.42	0.82	1.92	2.52	3.10	0.67
Co	0.56	1.87	2.85	3.22	4.42	4.56	1.44

Works of adhesion, W_{ad}, for 1/3 ML Cu and Co on the different Al_2O_3 surfaces, can be found in Table I. The W_{ad} is defined as the total energy of the alumina substrate and the isolated 1/3 ML of metal atoms, minus the total energy of the system, with the metals atoms adsorbed on the alumina surface, divided by the cross-sectional area. One can see that the W_{ad} of the metal/3(H-C)-terminated surface systems has the lowest values. Table I also indicates that the W_{ad} of 1/3 ML Co on each surface are higher than that of 1/3 ML Cu. That is, Co has a stronger interaction with the alumina surfaces than does Cu. These results are consistent with Fig. 3, i.e., that Cu will wet alumina when $\mu_{Cu} > -4.1$ eV, while Co will wet alumina for chemical potentials μ_{Co} as low as −5.9 eV.

Given the variety of wetting conditions that the six distinct alumina surfaces provide, as shown in Fig. 3, the different wetting conditions found experimentally[11,26–34] are perhaps not surprising. That is, one would expect the wetting to depend on the alumina surface H and C content, which in turn, depends on the sample processing and metal film growth environment.

In summary, an *ab initio* surface phase diagram for carbon and hydrogen on an $Al_2O_3(0001)$ surface was presented. Six types of distinct configurations for the surface were found. The Cu and Co metal wetting behavior and adhesion were found to depend sensitively on the C and H surface-state configuration. Our results could provide a reasonable framework for understanding and predicting the alumina surface structure and wetting behavior of metal deposition on alumina.

The authors gratefully acknowledge ONR support under Grant No. N00014-99-1-0170.

[1] J. Toofan and P. R. Watson, Surf. Sci. **401**, 162 (1998).
[2] J. Ahn and J. W. Rabalais, Surf. Sci. **388**, 121 (1997).
[3] P. J. Eng, T. P. Trainor, G. E. Brown, Jr., G. A. Waychunas, M. Newville, S. R. Sutton, and M. L. Rivers, Science **288**, 1029 (2000).
[4] K. C. Hass, W. F. Schneider, A. Curionl, and W. Andreoni, Science **282**, 265 (1998).
[5] Xiao-Gang Wang, Anne Chaka, and Matthias Scheffler, Phys. Rev. Lett. **84**, 3650 (2000).
[6] I. G. Batyrev, A. Alavi, and M. W. Finnis, Phys. Rev. B **62**, 4698 (2000).
[7] P. D. Tepesch, and A. A. Quong, Phys. Status Solidi B **217**, 377 (2000).
[8] E. A. Soares, M. A. Van Hove, C. F. Walters, and K. F. McCarty, Phys. Rev. B **65**, 195405 (2002).
[9] W. Zhang, and J. R. Smith, Phys. Rev. Lett. **85**, 3225 (2000).
[10] Xiao-Gang Wang, John R. Smith, and Matthias Scheffler, Phys. Rev. B **66**, 073411 (2002).
[11] S. A. Chambers, T. Droubay, D. R. Jennison, and T. R. Mattsson, Science **297**, 827 (2002).
[12] W. Zhang, and J. R. Smith, Phys. Rev. B **61**, 16 883 (2000).
[13] C. Niu, K. Shepherd, D. Martini, J. Tong, J. A. Kelber, D. R. Jennison, and A. Bogicevic, Surf. Sci. **465**, 163 (2000).
[14] Z. Lodziana, J. K. Noskov, and P. Stoltze, J. Chem. Phys. **118**, 11179 (2003).
[15] R. Di Felice and J. E. Northrup, Phys. Rev. B **60**, R16 287 (1999).
[16] K. Reuter and M. Scheffler, Phys. Rev. B **65**, 035406 (2001).
[17] B. Dillmann, F. Rohr, O. Seiferth, G. Klivenyi, M. Bender, K. Homann, I. N. Yakovkin, D. Ehrlich, M. Baumer, H. Kuhlenbeck, and H.-J. Freund, Faraday Discuss. **105**, 295 (1996).
[18] J. P. Perdew, K. Burke, and M. Ernzerhof, Phys. Rev. Lett. **77**, 3865 (1996).
[19] P. Blaha, K. Schwarz, P. I. Sorantin, and S. B. Trickey, Comput. Phys. Commun. **59**, 399 (1990).
[20] B. Kohler, S. Wilke, M. Scheffler, R. Kouba, and C. Ambrosch-Draxl, Comput. Phys. Commun. **94**, 31 (1996).
[21] M. Petersen, F. Wagner, L. Hufnagel, M. Scheffler, P. Blaha, and K. Schwarz, Comput. Phys. Commun. **126**, 294 (2000).
[22] The FP-LAPW numerical parameters are: $E_{max}^{wf}=18$ Ry, $R_{Al}^{MT}=0.90$, $R_{O}^{MT}=0.69$, $R_{H}^{MT}=0.21$, $R_{C}^{MT}=0.53$, $R_{Cu}^{MT}=0.95$, $R_{Co}^{MT}=0.95$ Å. A uniform k-point mesh with five points in the irreducible part of the Brillouin zone is used.
[23] J. R. Smith and W. Zhang, Acta Mater. **48**, 4395 (2000).
[24] X.-G. Wang, J. R. Smith, and A. Evans, Phys. Rev. Lett. **89**, 286102 (2002).
[25] U. Alber, H. Mullejans, and M. Ruhle, Micron **30**, 101 (1999).
[26] S. Varma, G. S. Chottiner, and M. Arbab, J. Vac. Sci. Technol. A **10**, 2857 (1992).
[27] J. G. Chen, M. L. Colaianni, W. H. Weinberg, and J. T. Yates, Jr., Surf. Sci. **279**, 223 (1992).
[28] F. S. Ohuchi, R. H. French, and R. V. Kasowski, J. Appl. Phys. **62**, 2286 (1987).
[29] G. Dehm, M. Ruhle, G. Ding, and R. Raj, Philos. Mag. B **71**, 1111 (1995).
[30] Y. Wu, E. Garfunkel, and T. E. Madey, J. Vac. Sci. Technol. A **14**, 1662 (1996).
[31] S. Gota, M. Gautier, L. Douillard, N. Thromat, J. P. Duraud, and P. Le Fevre, Surf. Sci. **323**, 163 (1995).
[32] M. Gautier, L. P. Van, and J. P. Duraup, Europhys. Lett. **18**, 175 (1992).
[33] A. F. Carley, M. K. Rajumon, and M. W. Roberts, J. Solid State Chem. **106**, 156 (1993).
[34] M. Baumer, and H.-J. Freund, Prog. Surf. Sci. **61**, 127 (1999).
[35] D. R. Jennison and T. R. Mattsson, Surf. Sci. Lett. **544**, L689 (2003).
[36] R. Franchy, Surf. Sci. Rep. **38**, 195 (2000).